[1]*Chemical Applications of Mössbauer Spectroscopy*, edited by V. I. Goldanskii and R. H. Herber (Academic, New York, 1968); G. M. Kalvius, in *Hyperfine Interactions in Excited Nuclei*, edited by G. Goldring and R. Kalish (Academic, New York, 1972), p. 523.
[2]E. Simanek and Z. Sroubek, Phys. Rev. **163,** 275 (1967); E. Simanek and A. Y. C. Wong, Phys. Rev. **166,** 348 (1968).
[3]R. R. Sharma, Phys. Rev. Lett. **26,** 563 (1971).
[4]G. A. Sawatzky and Julieke Hupkes, Phys. Rev. Lett. **25,** 100 (1970).
[5]J. E. Inglesfield, J. Phys. Chem. Solids **31,** 1435 (1970).
[6]J. C. Phillips, J. Phys. Chem. Solids **11,** 226 (1959).
[7]L. R. Walker, G. K. Wertheim, and V. Jaccarino, Phys. Rev. Lett. **6,** 98 (1961).
[8]J. Blomquist, B. Roos, and M. Sundbom, J. Chem. Phys. **55,** 141 (1971).
[9]P. H. Barrett and T. K. McNab, Phys. Rev. Lett. **25,** 1601 (1970). Very recently, a second resonance attributed to Fe^{+} has been found using $^{57}Co/^{57}Fe$ mixtures, Phys. Rev. Lett. **28,** 1547 (1972).
[10]T. K. McNab, H. Micklitz, and P. H. Barrett, Phys. Rev. B **4,** 3787 (1971).
[11]H. Micklitz and P. H. Barrett, Phys. Rev. B **5,** 1704 (1972).
[12]D. M. Mann and H. P. Broida, J. Chem. Phys. **55,** 84 (1971), and references contained therein.
[13]P. O. Löwdin, Phys. Rev. **97,** 1490 (1955).
[14]J. C. Slater, *Quantum Theory of Molecules and Solids* (McGraw-Hill, New York, 1963), Vol. 1, p. 315.
[15]E. Clementi, IBM J. Res. Dev. Suppl. **9,** 2 (1965).
[16]G. L. Pollack, Rev. Mod. Phys. **36,** 748 (1964).
[17]J. C. Slater, Phys. Rev. **81,** 385 (1951). The Slater-exchange approximation and the resulting HFS model have of course been in general use in energy-band theory for many years. Recently, numerical techniques have been developed for applying this model to molecular systems; e.g., the multiple-scattering technique; J. C. Slater and K. H. Johnson, Phys. Rev. B **5,** 844 (1972), and references therein; and the discrete variational method; see Ref. 18.
[18]D. E. Ellis and T. Parameswaran, Int. J. Quantum Chem. Symp. **5,** 443 (1971); D. E. Ellis, Int. J. Quantum Chem. Symp. **2,** 35 (1968).
[19]R. Ruegsegger and W. Kundig, Phys. Lett. B **39,** 620 (1972).

PHYSICAL REVIEW B VOLUME 7, NUMBER 3 1 FEBRUARY 1973

Correlated Electron Paramagnetic Resonance and Optical Study of $CdF_2:Er^{3+}$. II. C_{3v} Local-Site Symmetry

T. C. Ensign and N. E. Byer
Research Institute for Advanced Studies, Martin Marietta Corporation, 1450 South Rolling Road, Baltimore, Maryland 21227
(Received 5 September 1972)

A high concentration of a single type of trigonal Er^{3+} site has been generated in CdF_2:Er crystals that were fired in oxygen subsequent to growth. More than 86% of the *noncubic* Er^{3+} sites observed were found by EPR measurements to be in trigonal sites with g values ($g_{||}=2.875$ and $g_{\perp}=8.344$) similar to those for the C_{3v}(II) spectrum examined by Ranon and Low in CaF_2:Er. This selective generation of C_{3v}(II) sites has permitted an unambiguous determination of the structure of the $^4I_{15/2}$ ground state of Er^{3+} ions residing in these sites, using low-temperature optical-absorption and -emission data. The crystal field splitting of the $^4I_{15/2}$ multiplet in C_{3v} symmetry is in reasonably good agreement with that expected from the cubic-field approximation of Lea, Leask, and Wolf for crystal field parameters $A_4\langle r^4\rangle=-226$ cm^{-1} and $A_6\langle r^6\rangle=37$ cm^{-1}. Cd-vapor and water-vapor treatments were found to generate not only the C_{3v}(II) site, but also a C_{3v}(I) site ($g_{||}=3.231$ and $g_{\perp}=8.344$). Vacuum treatment was found to lead to the C_{3v}(I) site only. The implications of this study in terms of recently proposed models for oxygen-compensated (trigonal) rare-earth-ion sites are discussed.

I. INTRODUCTION

Recently, correlated electron paramagnetic resonance (EPR) and optical studies of Er^{3+} in crystals of CdF_2, space group O_h^5 ($Fm3m$), have permitted an unambiguous characterization of the orthorhombic (C_{2v}) Er^{3+} lattice sites that form as a result of the trivalent rare-earth ion being charge compensated locally with a monovalent cation (Li^+, Na^+, Ag^+, or K^+).[1] Those studies[1] (hereafter denoted I) and others[2–4] were concerned with both the crystal field and the optical properties of C_{2v} Er^{3+} sites in CdF_2. Similar investigations have been performed on CdF_2 crystals containing Er^{3+} ions in trigonal sites, and selected results of these measurements, especially those related to the Er infrared quantum counter, have been reported elsewhere.[3–6] The EPR, optical-absorption, and luminescence results presented in this paper have allowed the detailed characterization of a C_{3v} Er^{3+} site, designated C_{3v}(II), that was generated by firing $CdF_2:Er^{3+}$ crystals in oxygen subsequent to their growth. In particular, the structure of the $^4I_{15/2}$ ground state of Er^{3+} has been determined for this site. Another C_{3v} Er^{3+} center, designated C_{3v}(I), was generated by various different thermal treatments. The experimental details and results are presented in Secs. II and III, respectively, the crystal field discussion appears in Sec. IV, and the implications of these results on recently proposed models for oxygen-compensated (trigonal) rare-earth-ion sites are discussed in Sec. V.

TABLE I. Relative concentration of trigonal Er^{3+} sites for differently prepared CdF_2: Er^{3+} crystals.

Crystal treatment	Trigonal Er^{3+} sites (%)[a] C_{3v}(I)	C_{3v}(II)
Vacuum	100	•••
Cd vapor	33	67
Water vapor	33	67
Oxygen	•••	100

[a]Magnitude of the *total* concentration of trigonal Er^{3+} sites depends upon the particular crystal treatment used (see text).

II. EXPERIMENTAL

A. Sample Preparation

It is well established for crystals exhibiting the fluorite lattice structure that charge compensation of trivalent rare-earth-ion dopants can be achieved in a variety of ways. In this study we report results for Er^{3+} ions in CdF_2 single crystals in which these dopant ions are located primarily in trigonal sites. All CdF_2: Er^{3+} specimens discussed in this paper contain 0.1-mole% ErF_3 and have been grown under similar conditions.[4,7] Four different methods of sample preparation subsequent to crystal growth have been employed on specimens approximately $1\times3\times7$ mm: (i) oxygen, (ii) water vapor, (iii) Cd vapor, and (iv) vacuum treatments. Each of these techniques has been found to generate trigonal Er^{3+} sites. The experimental procedure followed for the water-vapor treatment was nearly identical to that used for oxygen firing.[4] For the oxygen treatment, the specimen was fired at 800 °C in 1 atm of gas for periods of time as long as 20 h; for the water treatment, only a partial pressure (~ 5 Torr) of water vapor was admitted to the quartz sample tube, and the treatment duration was reduced to about 20 min, again at 800 °C. This procedure limited the buildup of a CdO coating[4,8,9] on the crystal surface, which had been found to cause brittleness in the samples. This conductive CdO coating was removed carefully from water-treated specimens before making any measurements. The method of Cd-vapor treatment used in this study was similar to that commonly employed to convert certain rare-earth-doped CdF_2 crystals to the semiconducting state.[10] The Pyrex tube containing the sample and Cd metal was evacuated (~ 4×10^{-6} Torr) prior to being sealed off. The Cd treatment proceeded at 550 °C for 1 h, after which time the sample was cooled rapidly to room temperature by removing the tube from the furnace. The vacuum-treated samples were heated at 550 °C for approximately 4 h in a vacuum of 4×10^{-7} Torr before being quenched.

B. EPR and Optical Studies

EPR spectra were obtained at 4.2 K for the magnetic field in a {110} crystalline plane using a conventional X-band spectrometer described in I. Photoluminescence measurements were made at 77 and 4.2 K. Absorption data were obtained at about 80 K using a cold-finger Dewar. The procedure used for both the absorption and luminescence experiments is the same as that discussed in detail in I.

III. RESULTS

A. EPR

The angular variation of the EPR spectrum of CdF_2: Er^{3+} samples prepared as described in Sec. II show the presence of two dominant noncubic Er^{3+} sites, both with trigonal symmetry. These sites are designated C_{3v}(I) and C_{3v}(II), and their relative concentration after each treatment is provided in Table I. The magnitude of the *total* concentration of trigonal Er^{3+} sites depends upon the particular crystal treatment used and was observed to be the smallest for the vacuum treatment, increasing progressively with Cd-vapor and then water-vapor treatments. The total concentration of Er^{3+} in trigonal sites was found to be the greatest for specimens of CdF_2 that were fired in oxygen for 20 h. More than 86% of the Er^{3+} ions that reside in *noncubic* lattice sites of oxygen-fired crystals reside in C_{3v}(II) sites (cf. Table II).

The g values obtained in this work for Er^{3+} ions in O_h and C_{3v} symmetry in CdF_2 are summarized in Table III. For comparison, g values measured for cubic and trigonal Er^{3+} sites in other fluorite crystals are listed also.[11,12] It is significant that the C_{3v}(I) and C_{3v}(II) centers in CdF_2 and CaF_2 have similar g values, which differ from those of the single C_{3v} site observed in SrF_2 and BaF_2. The C_{3v} site in SrF_2 and BaF_2 is believed to arise from a next-nearest-neighbor fluorine interstitial.[12,13]

TABLE II. Relative distribution of Er^{3+} sites after oxygen-firing CdE_2 specimens for different periods of time.

Oxygen treatment (h)	Er^{3+} sites (%)[a] Cubic O_h	Trigonal[b] C_{3v}(II)	Other noncubic[c]
0	75	•••	25
3	58	25	17
20	7	80	13

[a]Uncertainties in the relative distribution are approximately ±10% of the tabulated values.

[b]No C_{3v}(I) Er^{3+} sites were observed after oxygen firing.

[c]Symmetry of the "other" noncubic sites has not been determined (see text).

TABLE III. g values observed for Er^{3+} in cubic and trigonal sites in CdF_2, CaF_2, SrF_2, and BaF_2.

Crystal	Site symmetry	$g_{\parallel}$	$g_{\perp}$	$\frac{1}{3}\mathrm{Tr}\{g\}$
CdF_2[a]	O_h	6.759	6.759	6.759
	C_{3v}(I)	3.231	8.334	6.633
	C_{3v}(II)	2.875	8.334	6.514
CaF_2[b]	O_h	6.785	6.785	6.785
	C_{3v}(I)	3.30	8.54	6.79
	C_{3v}(II)	2.206	8.843	6.631
SrF_2[c]	O_h	6.803	6.803	6.803
	C_{3v}	6.179	7.054	6.762
BaF_2[c]	O_h	6.755	6.755	6.755
	C_{3v}	5.94	7.13	6.73

[a]This work. Uncertainties in the g values are ± 0.005.
[b]Reference 11.
[c]Reference 12.

The larger g-value anisotropy in CdF_2, as in CaF_2,[11] is consistent with both trigonal Er^{3+} sites arising from nearest-neighbor charge compensation.

The EPR linewidths measured at 4.2 K for the C_{3v}(I) and C_{3v}(II) Er^{3+} centers in CdF_2 were ~14 and ~21 G, respectively, for the magnetic field parallel to a ⟨111⟩ crystal axis. No fine structure was observed for any crystal orientation.

In Table II, the relative distribution of O_h and C_{3v}(II) Er^{3+} sites is listed for CdF_2 specimens that were fired in oxygen for different durations. The tabulated percentages were obtained from the total integrated-EPR absorption intensity for the magnetic field parallel to a ⟨111⟩ crystal axis. It should be noted that the EPR spectra corresponding to the "other" noncubic Er^{3+} sites varied depending upon the treatment time; unfortunately, these spectra were weak and frequently very anisotropic, making the identification of site symmetry impossible. Tables I and II reveal, however, that oxygen firing generates only one type of trigonal center, C_{3v}(II), independent of the treatment period. In contrast, both the C_{3v}(I) and C_{3v}(II) centers are present subsequent to water- or Cd-vapor treatment (Table I).

B. Low-Temperature Optical Spectra

The above EPR results have established that a high concentration of a single type of noncubic Er^{3+} site is generated by oxygen firing specimens of CdF_2:Er. The selective generation of Er^{3+} sites has allowed the optical properties of these specimens to be correlated unambiguously with a particular Er^{3+} site, i.e., the C_{3v}(II) site.

1. $^4S_{3/2} \rightleftarrows {}^4I_{15/2}$ *Spectra*

Low-temperature emission spectra (77 and 4.2 K) and absorption spectra (~80 K), obtained for the $^4S_{3/2} \rightleftarrows {}^4I_{15/2}$ transition of Er^{3+} in oxygen-fired CdF_2, i.e., CdF_2: (Er^{3+}, O^{2-}), have been used to determine the Er^{3+} $^4I_{15/2}$ crystal field splitting. The $^4S_{3/2}$ multiplet is the simplest electronic state of Er^{3+}, consisting of two levels in a trigonal crystal field. The $^4I_{15/2}$ ground-state multiplet has eight levels in C_{3v} symmetry (cf. Sec. IV). The $^4S_{3/2} \rightarrow {}^4I_{15/2}$ emission spectrum obtained at 77 K is shown in Fig. 1. Selective excitation studies indicate that this spectrum originates from at least two different Er^{3+} sites. The numbered lines have a $^4I_{15/2} \rightarrow {}^2H_{11/2}$ excitation band centered at 515 nm and have been attributed to Er^{3+} in C_{3v}(II) sites. The weaker Er^{3+} emission lines, the majority of which are observed in the region $18\,300 \pm 200$ cm^{-1}, have a $^4I_{15/2} \rightarrow {}^2H_{11/2}$ excitation band centered at 520 nm. Most of these transitions are located at energies corresponding to lines in the CdF_2: (Er^{3+}, U) emission spectrum (see Fig. 6 of I). The presence of these additional emission lines is consistent with the evidence for Er^{3+} in sites other than C_{3v}(II) provided by the EPR results shown in Table II.

As in the case of Er^{3+} in C_{2v} symmetry (see I), several of the broader lines in Fig. 1 may arise from the vibronic emission associated with the numbered sharp electronic lines. An analysis of this aspect of Fig. 1 has not been made.

Luminescence data, obtained for CdF_2: (Er^{3+}, O^{2-}) specimens, show that the emission lines designated by a prime in Fig. 1 disappear at 4.2 K. The absorption spectra of these crystals reveal that the strengths of lines corresponding in energy to emission lines 1 and 1′ are unchanged in cooling the specimens from 295 to ~80 K, while all the other lines decrease in strength. These observations are consistent with the fact that there are only two $^4S_{3/2}$ levels and the upper levels of the $^4I_{15/2}$ multiplet are depopulated at low temperatures. Therefore, the luminescence, absorption, and EPR results confirm conclusively that the group of numbered lines in Fig. 1 are produced by one type of Er^{3+} site, i.e., the C_{3v}(II) site.

2. $^4I_{15/2}$ *Crystal Field Splitting*

As illustrated in Fig. 1, the $^4S_{3/2} \rightarrow {}^4I_{15/2}$ emission spectrum arising from Er^{3+} in C_{3v}(II) symmetry consists of two series of eight lines each. A primed series 1′, 2′, ..., 8′ corresponds to transitions from the upper level, $E2$, of the $^4S_{3/2}$ multiplet to the $Z1$, $Z2$, ..., $Z8$ levels of the $^4I_{15/2}$ ground state, respectively. Similarly, the unprimed series results from decay of the lower $^4S_{3/2}$ level, $E1$, to the $^4I_{15/2}$ multiplet. In Table IV, the wave numbers of the two series of lines are listed, and the energies $E(Zi)$ in cm^{-1} are given by the average of $(\bar{\nu}_1 - \bar{\nu}_i)$ and $(\bar{\nu}_{1'} - \bar{\nu}_{i'})$.

IV. CRYSTAL FIELD

EPR studies of CdF_2: (Er^{3+}, O^{2-}) crystals indicate that charge compensation of the Er^{3+} ion leads

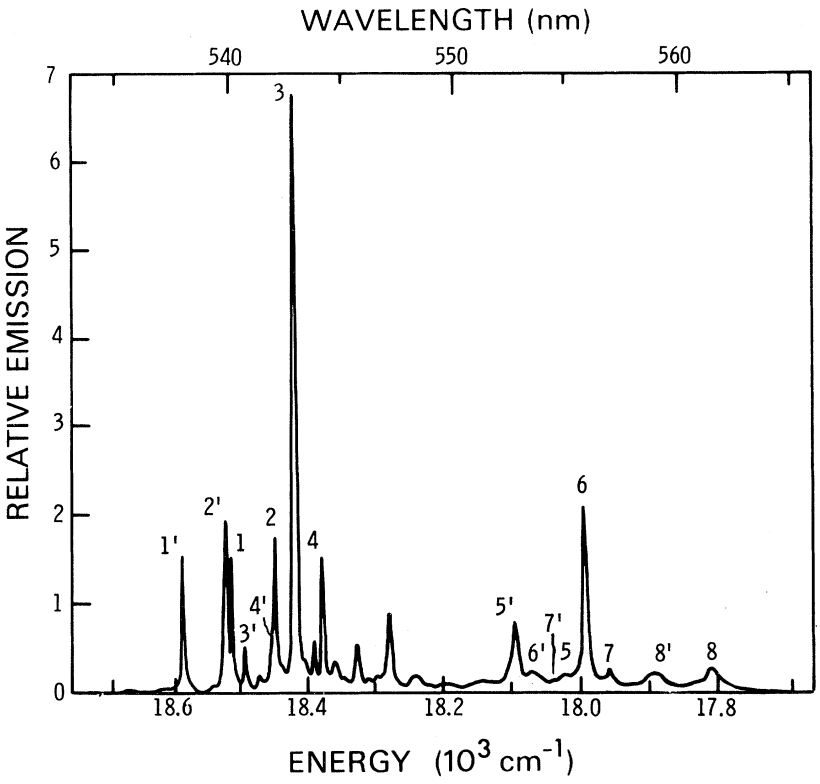

FIG. 1. Emission spectrum, obtained at 77 K, for the $^4S_{3/2} \rightarrow {}^4I_{15/2}$ transition in CdF_2: (Er^{3+}, O^{2-}). The electronic lines that are numbered are identified in the text.

to the formation of a single type of trigonal site that accounts for nearly all of the noncubic sites present in samples prepared by oxygen firing. In the following discussion, the EPR and optical properties of the C_{3v}(II) Er^{3+} site reported in Sec. III are analyzed on the basis of a point-charge crystal field approximation.

For this purpose, the formalism of Lea, Leask, and Wolf (LLW)[14] has been employed in a manner similar to that used previously in I to describe the interaction of the $^4I_{15/2}$ ground state of the Er^{3+} ion with the cubic component of the crystal field. The g values obtained from EPR spectra of Er^{3+} in C_{3v}(II) sites (Table III) suggest that x, a parameter related to the ratio of the fourth- and sixth-order cubic field terms, lies between -0.46 and 0. An x value within these limits predicts a distribution of $^4I_{15/2}$ energy levels consistent with that obtained from the $^4S_{3/2} \rightarrow {}^4I_{15/2}$ luminescence spectra recorded in Table IV and depicted in Fig. 1. The parameter x and the energy scale factor W, defined by LLW, have been obtained from the optical data in the following way. From Table IV, it is seen that energy levels $Z2$, $Z3$, and $Z4$ are separated by ~70 cm^{-1} and lie ~360 cm^{-1} below the levels $Z5$, $Z6$, $Z7$, and $Z8$. We have assumed that the interaction between these two groups of levels and the interaction of either of these two groups with the ground state (level $Z1$) is negligible. In this approximation, it is reasonable to use the average $E(Zi)$ for each of these groups, namely, 98.2 cm^{-1} for the intermediate group and 568.2 cm^{-1} for the upper group, to calculate x and W. The values obtained in this manner, $x = -0.36$ and $W = 1.67$ cm^{-1}, are seen to be very nearly the same as those found in I for the C_{2v}(Er^{3+}, M^+) center, i.e., $x = -0.36$ and $W = 1.810$ cm^{-1}. The energies predicted from LLW, using these values of x and W are compared with the experimental numbers in Fig. 2, which also shows the

TABLE IV. Crystal field splitting of the $^4I_{15/2}$ ground state of (Er^{3+}, O^{2-}). $E(Zi)$ were calculated from the luminescence spectrum of the $^4S_{3/2} \rightarrow {}^4I_{15/2}$ transition at 77 K.

Energy level	$\bar{\nu}$[a] (cm^{-1})	$\bar{\nu}'$[a] (cm^{-1})	$E(Zi)$[b] (cm^{-1})
$Z1$	18 510.5	18 585.6	0
$Z2$	18 445.3	18 519.9	65.5
$Z3$	18 417.0	18 492.4	93.4
$Z4$	18 374.7	18 450.0	135.7
$Z5$	(18 018.0)	18 091.0	494.6
$Z6$	17 989.3	18 062.4	522.2
$Z7$	17 055.9	(18 032.3)	554.6
$Z8$	17 809.1	(17 889.7)	701.4

[a] $\bar{\nu}$ and $\bar{\nu}'$ correspond to the wave numbers in air; parentheses indicate where uncertainties exist (e.g., arising from line broadening).

[b] Uncertainty in $E(Zi)$ is ± 0.4 cm^{-1}.

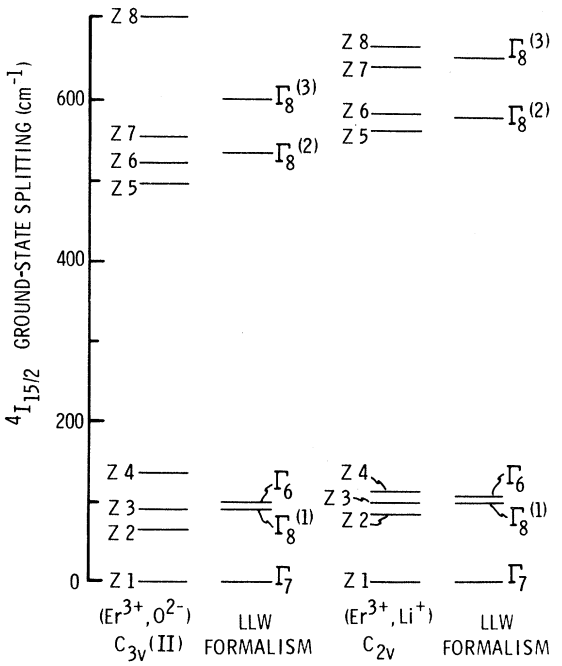

FIG. 2. $^4I_{15/2}$ ground-state splitting determined experimentally for (Er^{3+}, O^{2-}) and (Er^{3+}, Li^{+}) centers in CdF_2 and calculated using the cubic-field approximation of Lea, Leask, and Wolf (Ref. 14).

results from I for (Er^{3+}, Li^{+}). The axial field for the C_{3v}(II) site is much stronger than for the C_{2v} site, as evidenced by the greater splitting of the Γ_8 states in a trigonal field (Fig. 2) and the larger g-value anisotropy (Table III). Nevertheless, the cubic approximation is successful in predicting the relative distribution of the experimentally determined $^4I_{15/2}$ energy levels. Using the above values of x and W, the fourth- and sixth-order cubic crystal field parameters for CdF_2: (Er^{3+}, O^{2-}) are found to be $A_4\langle r^4\rangle = -226$ cm^{-1} and $A_6\langle r^6\rangle = 37$ cm^{-1}, remarkably close to the values found for the C_{2v} (Er^{3+}, M^{+}) site ($A_4\langle r^4\rangle = -245$ cm^{-1} and $A_6\langle r^6\rangle = 40$ cm^{-1}).

V. MODELS

More information concerning the nature of the C_{3v}(II) Er^{3+} site in CdF_2 can be obtained by comparing results for rare-earth ions on trigonal sites in other crystals that have the fluorite structure. Ranon and Low's[11] investigation of Er^{3+} in CaF_2 suggests that the g values obtained for the C_{3v}(II) site in this study arise from the structure (Er^{3+}-F_7^--O^{2-}) depicted in Fig. 3(a). Recent electron nuclear double resonance (ENDOR) studies[15] of Yb^{3+} and Ce^{3+} in CaF_2 indicate, however, that the C_{3v}(Er^{3+}, O^{2-}) site identified by Ranon and Low may have the structure (Er^{3+}-F^--O_4^{2-}) shown in Fig. 3(b). Moreover, it appears possible that the simple (Er^{3+}-F_7^--O^{2-}) structure need not form before the more complex (Er^{3+}-F^--O_4^{2-}) structure; the latter may be present in as-grown material under suitable circumstances.[15] Because each of these two structures is expected to generate a similar crystal field at the Er^{3+} ion, some uncertainty remains regarding the configuration of the C_{3v}(II) site generated in CdF_2: Er by oxygen firing. In particular, if the four O^{2-} ions are distributed in the intuitively most obvious fashion shown in Fig. 3(b), they form a regular tetrahedron on four of the eight vertices of the cube. The trigonal environment, then, is seen to be a superposition of the field due to the tetrahedron of oxygen ions and an axial field along a $\langle 111\rangle$ direction arising from the single F^- ion. Within the framework of the point-charge crystal field model, the signs and magnitudes of $A_4\langle r^4\rangle$ and $A_6\langle r^6\rangle$ (i.e., the even parity part of the potential) for a cube of eight singly charged fluorine ions are equal to those for a tetrahedron of four doubly charged oxygen ions at the same nearest-neighbor distances. Thus, $x(T_d) = x(O_h)$ and $W(T_d) = W(O_h)$. Both of the models for the C_{3v} (Er^{3+}, O^{2-}) site shown in Fig. 3 appear, therefore, to be consistent with the results of the crystal field analysis presented above.

Additional evidence, however, suggests that the C_{3v}(II) Er^{3+} site may possess the (Er^{3+}-F^--O_4^{2-}) structure. It is noteworthy that in this study the C_{3v}(II) Er^{3+} center is generated as the sole trigonal site only under the controlled conditions of oxygen firing (see Tables I and II). These conditions are

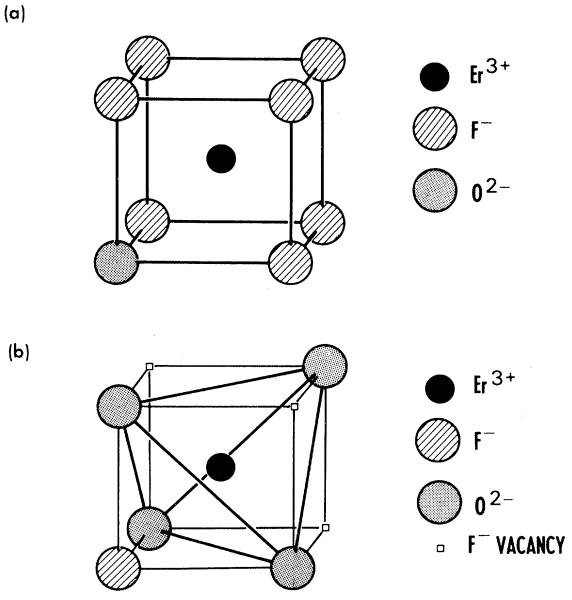

FIG. 3. Possible models for the C_{3v} Er^{3+} sites in CdF_2: (a) the (Er^{3+}-F_7^--O^{2-}) structure and (b) the (Er^{3+}-F^--O_4^{2-}) structure.

similar to those necessary to obtain the (Er^{3+}-F^--O_4^{2-}) structure in as-grown (Czochralski) CaF_2: Yb^{3+} and Ce^{3+} [15] in that a substantial partial pressure of oxygen is present during growth. In addition, Ranon and Low's[11] technique to form trigonal Er^{3+} sites in CaF_2 subsequent to growth appears to be closely similar to that employed on Ce^{3+} and Yb^{3+} in CaF_2 where the sites were identified by ENDOR.[15] Therefore, the sequence of centers that result is expected to be the same, suggesting that Ranon and Low's C_{3v}(I) site has the (Er^{3+}-F_7^--O^{2-}) structure and that their C_{3v}(II) site possesses the (Er^{3+}-F^--O_4^{2-}) structure. The g values corresponding to the C_{3v}(I) and C_{3v}(II) sites in CdF_2 (Table II) are very similar to those obtained for the respective Er^{3+} sites in CaF_2. These results suggest that in CdF_2 the C_{3v}(II) Er^{3+} site has the (Er^{3+}-F^--O_4^{2-}) structure and that the C_{3v}(I) site possesses the (Er^{3+} – F_7^--O^{2-}) or perhaps the (Er^{3+}-H^--O_4^{2-}) structure.[15] Both of the models shown in Fig. 3 should exhibit similar superhyperfine structure in their EPR spectra, which would differ in this respect from the spectrum of the (Er^{3+}-H^--O_4^{2-}) center. Unfortunately, the breadth of the Er^{3+} EPR lines (Sec. III) masked the possible presence of a doublet structure for the magnetic field along a ⟨111⟩ direction, which prohibited distinguishing between the two kinds of sites on this basis.

VI. SUMMARY

It has been shown that the cubic-field approximation accounts reasonably well for the luminescence data arising from Er^{3+} in a trigonal site in CdF_2, especially in that the LLW formalism predicts the observed distribution of the $^4I_{15/2}$ ground-state energy levels. The cubic component of the crystalline field at the C_{3v}(II) site has been found to be very similar to that at the C_{2v} site (i.e., the fourth- and sixth-order cubic terms are approximately the same for both sites). An axial-field perturbation along a ⟨111⟩ direction is consistent with the anisotropy of the EPR g values, and the magnitude of the Γ_8 splittings (see Fig. 2) indicates that the axial component of the crystal field is large for the C_{3v}(Er^{3+}, O^{2-}) site as compared to the C_{2v}(Er^{3+}, Li^+) site.

Both of the models for the C_{3v}(Er^{3+}, O^{2-}) site shown in Fig. 3 have been shown to be consistent with the crystal field parameters. The unequivocal verification of the mode of charge compensation must await an ENDOR investigation of the CdF_2: (Er^{3+}, O^{2-}) crystals employed in this study, or of crystals prepared under identical conditions.

ACKNOWLEDGMENTS

The authors wish to thank W. R. Hosler of the Solid State Physics Section at the National Bureau of Standards for the CdF_2 crystals used in this study. The assistance of R. G. Lye, W. M. Mularie, and S. E. Stokowski of the Physics Department at the Research Institute for Advanced Studies and their critical analyses of this paper also have been most beneficial. We are grateful to W. Holton for performing many of the measurements, and to J. Minnucci for his assistance in treating the samples.

[1]T. C. Ensign and N. E. Byer, Phys. Rev. B **6,** 3227 (1972).

[2]T. C. Ensign, N. E. Byer, and W. M. Mularie, Bull. Am. Phys. Soc. **17,** 310 (1972).

[3]N. E. Byer, T. C. Ensign, and W. M. Mularie, in *Proceedings of the IRIS (Detector Specialty Group), March 1972* (The Infrared Information and Analysis Center, The University of Michigan Press, Ann Arbor, Mich., to be published).

[4]N. E. Byer, T. C. Ensign, W. M. Mularie, and S. E. Stokowski, J. Appl. Phys. (to be published).

[5]N. E. Byer, T. C. Ensign, and W. M. Mularie, Appl. Phys. Lett. **20,** 286 (1972).

[6]N. E. Byer, T. C. Ensign, and W. M. Mularie, Bull. Am. Phys. Soc. **17,** 310 (1972).

[7]W. R. Hosler, Natl. Bur. Stds., Washington, D. C. (unpublished).

[8]The CdO coating was identified through its characteristic x-ray diffraction pattern using the powder technique of Debye and Scherrer.

[9]J. M. Moret, J. Weber, and R. Lacroix, Helv. Phys. Acta **41,** 243 (1968).

[10]J. D. Kingsley and J. S. Prener, Phys. Rev. Lett. **8,** 315 (1962).

[11]U. Ranon and W. Low, Phys. Rev. **132,** 1609 (1963).

[12]A. A. Antipin, I. N. Kurkin, L. D. Livanova, L. Z. Potvorova, and L. Ya Shekun, Fiz. Tverd. Tela **8,** 2664 (1966) [Sov. Phys.-Solid State **8,** 2130 (1967)].

[13]M. R. Brown, K. G. Roots, J. M. Williams, W. A. Shand, C. Groter, and H. F. Kay, J. Chem. Phys. **50,** 891 (1969).

[14]K. R. Lea, M. J. Leask, and W. P. Wolf, J. Phys. Chem. Solids **23,** 1381 (1962).

[15]T. Rs. Reddy, E. R. Davies, J. M. Baker, D. N. Chambers, R. C. Newman, and B. Özbay, Phys. Lett. A **36,** 231 (1971); D. N. Chambers, Phys. Lett. A **37,** 77 (1971); D. N. Chambers and R. C. Newman, J. Phys. C **4,** 3015 (1971); **5,** 997 (1972).